An organotrophic *Sideroxydans* reveals potential iron oxidation marker genes

Rene L. Hoover[1,2], Kirsten Küsel[3,4], Clara S. Chan[1,2,5]

1 Microbiology Graduate Program, University of Delaware, Newark, Delaware, USA
2 Department of Earth Sciences, University of Delaware, Newark, Delaware, USA
3 Aquatic Geomicrobiology, Institute of Biodiversity, Friedrich Schiller University, Jena, Germany
4 Cluster of Excellence Balance of the Microverse, Friedrich Schiller University, Jena, Germany
5 School of Marine Science and Policy, University of Delaware, Newark, Delaware, USA

Abstract

To understand the ecophysiology and the role of iron-oxidizing bacteria (FeOB) in various ecosystems, we need to identify marker genes of the iron oxidation pathway to track activity *in situ*. The Gallionellaceae *Sideroxydans* sp. CL21, an autotrophic iron-oxidizing bacteria isolated from a peatland, is unusual amongst FeOB isolates in its genomic potential to utilize organic compounds as energy sources. Thus, it offers the unique opportunity to elucidate which genes are expressed under litho- versus organotrophic conditions. We demonstrated the growth of *Sideroxydans* sp. CL21 on organic substrates (lactate and pyruvate) and inorganic substrates (Fe(II), magnetite, thiosulfate, and S(0)). Thus, cells were capable of lithoautotrophic, organotrophic, and potentially organoheterotrophic growth. Surprisingly, when lactate-grown cells were given Fe(II), mid-log phase cells were unable to oxidize iron, while late-log phase cells oxidized iron. To elucidate iron oxidation pathways, we compared gene expression between mid-log (non-iron-oxidizing) and late-log (iron-oxidizing) lactate-grown cells. Genes for iron oxidases (*cyc2, mtoA*) were highly expressed at both time points, so did not correspond to iron oxidation capability, making them unsuitable marker genes of iron oxidation activity by themselves. However, genes encoding periplasmic and inner membrane cytochromes were significantly upregulated in cells capable of iron oxidation. These genes include *mtoD*, *cymA/imoA*, and a cluster of Fe(II)-responsive genes (*ircABCD*). These findings suggest Gallionellaceae regulate their iron oxidation pathways in multiple stages, with iron oxidase-encoding genes proactively expressed. Other genes encoding electron carriers are upregulated only when iron oxidation is needed, which makes these genes (i.e. *ircABCD*) good prospective indicators of iron oxidation ability.

Importance

FeOB are widespread in the environment and we suspect that they play key roles in nutrient and other elemental cycles. However, with no isotopic marker, we lack the ability to

monitor FeOB activity, prompting us to search for genetic markers. Previous work suggests that expression of iron oxidase genes does not correspond to iron oxidation activity in Gallionellaceae and little was known about the other genes in the pathway. Here we study a unique FeOB isolate that possesses organotrophic capabilities and demonstrate its potential for mixotrophic growth on lactate and Fe(II). Its ability to oxidize iron is regulated, allowing us to discover potential iron oxidation pathway genes with expression that corresponds to iron oxidation activity. If these genes can be further validated as iron oxidation marker genes, they will enable us to delineate autotrophic and organoheterotrophic FeOB impacts on carbon cycling in wetlands and other natural and engineered environments.

Introduction

Iron oxidation is a widespread process in the environment, playing key roles in water and soil health as Fe(III) oxyhydroxides can adsorb various nutrients and metals (1). Despite the pervasiveness and importance of iron oxidation, there remains much uncertainty as to how much of it is abiotic versus biotic, i.e. catalyzed by iron-oxidizing bacteria (FeOB). This distinction (biotic vs. abiotic) is key to understanding how iron oxidation affect other nutrient cycles, which requires 1) a deeper understanding of C metabolisms of FeOB and 2) a method to link microbial iron oxidation activity in the environment to C and other metabolic transformations. Although FeOB are widely thought to be primarily autotrophic, accumulating evidence suggests a considerable number of FeOB may be mixotrophic (2–6) or organo(hetero)trophic (7, 8), expanding their potential effects on C cycling. Because these FeOB can use alternate energy sources (9–12), they are not always oxidizing iron, so we require a method of detecting active iron oxidation. To link microbial iron oxidation to biogeochemical effects, we need gene markers of iron oxidation activity.

Studying facultative FeOB allows us to discern genes specific to iron oxidation. An isolate of the Gallionellaceae, *Sideroxydans* sp. CL21, presents a new opportunity to learn about FeOB metabolism, iron oxidation mechanisms, and potential marker genes. *Sideroxydans* sp. CL21 is rare amongst FeOB isolates in possessing genes for organoheterotrophy, notably lactate permease and dehydrogenase. It was isolated from the Schlöppnerbrunnen fen (13), a semi-acidic (pH 4.5 to 5.5), iron-rich peatland in Northern Germany (14–16). *Sideroxydans* sp. CL21 is closely related to the well-studied *Sideroxydans lithotrophicus* ES-1 (9), but differs from ES-1 in that its genome is ~20% larger and encodes genes for organoheterotrophy (17, 18). *Sideroxydans* sp. CL21 has been shown to grow on the non-iron substrates H_2 and thiosulfate (18). It has also been grown on the reduced iron substrates FeS and Fe(0) (13, 18), but neither of these are pure Fe(II) substrates as Fe(0) evolves H_2, so growth on Fe(II) alone has not been demonstrated. *Sideroxydans* sp. CL21 has also been grown in the presence of mixed substrates, including lactate/FeS and lactate/Fe(0) (13, 18). However, previous cultures did not grow on lactate alone (13, 18). Thus, while the growth in the presence of combined organic and inorganic electron

73 donors suggests a potential for mixotrophy, further work is needed to clarify exactly which
74 substrates promote *Sideroxydans* sp. CL21 growth and support organoheterotrophy.
75 Markers of iron oxidation activity could be the genes within iron oxidation pathways, but
76 our knowledge of these pathways is still in development. The *Sideroxydans* sp. CL21 genome
77 encodes several genes related to iron oxidation and associated pathways. Its genome encodes two
78 known iron oxidases, 1) the monoheme cytochrome-porin Cyc2 and 2) the decaheme
79 cytochrome MtoA and associated porin MtoB (17–19). In fact, the genome has three copies of
80 *cyc2* and an *mtoAB,* plus an additional copy of *mtoA* next to an unnamed porin. In the closely
81 related *Sideroxydans lithotrophicus* ES-1, one copy of *cyc2* is highly expressed in both iron-
82 oxidizing and thiosulfate-oxidizing cells, while the other two copies have low expression during
83 thiosulfate oxidation, but are upregulated when oxidizing iron (10). In marine hydrothermal
84 environments, the *cyc2* gene is highly expressed by various iron-oxidizing Zetaproteobacteria,
85 and expression increases in microcosms amended with Fe(II) (20). In the facultative FeOB
86 Zetaproteobacteria *Ghiorsea bivora* TAG-1, $cyc2_{TAG\text{-}1_1}$ and $Cyc2_{TAG\text{-}1_1}$ are expressed under
87 both H_2- and iron-oxidizing conditions (21). Together, this suggests *cyc2*/Cyc2 expression may
88 not necessarily correspond to iron oxidation activity. There is less information on
89 *mtoAB/*MtoAB, though these iron oxidase genes/proteins are upregulated in *S. lithotrophicus* ES-
90 1 grown on Fe(II) minerals (22, 23). *Sideroxydans* sp. CL21 also encodes two gene clusters,
91 predicted to encode porin-cytochrome complexes (PCC), each with two multiheme cytochromes
92 ($PCC3_{copy1}$, cytochromes have 24 and 14 hemes; $PCC3_{copy2}$, cytochromes have 24 and 12 hemes).
93 PCC3 is hypothesized to also play a role in extracellular electron transport and possibly iron
94 oxidation (24). Additional putative components of the iron oxidation pathway (*mtoD*,
95 *cymA/imoA*, Slit $1321\text{-}1324_{ES\text{-}1}$) are less well studied; these include genes for inner membrane
96 and periplasmic electron carriers. In all, *Sideroxydans* sp. CL21 has a wide variety of genes that
97 are known or predicted to participate in iron oxidation, giving multiple possibilities for marker
98 genes.
99 Here, we constrain potential iron oxidation marker genes by studying differential gene
100 expression in *Sideroxydans* sp. CL21. We first optimized the cultivation conditions by testing
101 *Sideroxydans* sp. CL21's growth on organic acids alone, plus other Fe(II) and non-iron
102 substrates. Cells grew quickly and to the highest cell density on organic acids. We then tested the
103 ability of these organic-grown cells to oxidize iron and found that lactate-grown cells exhibited a
104 difference in iron-oxidizing phenotype between mid-log (no iron oxidation activity) and late-log
105 (iron oxidation activity). This enabled us to compare gene expression between iron-oxidizing and
106 non-iron-oxidizing conditions to detect genes whose expression corresponds to iron oxidation
107 potential. The genes identified help expand our knowledge of the iron oxidation pathway and
108 provide a list of candidate marker genes for iron oxidation.

Results

Physiology and growth on Fe(II), S, and organic substrates

Sideroxydans sp. CL21 grew on a range of individual organic and inorganic electron donors (Fig. 1). *Sideroxydans* sp. CL21 grew well on dissolved, ferrous iron ($FeCl_2$), reaching a cell density of 1.25 x 10^7 cells/mL in 15 days (Fig. 1A). This growth on $FeCl_2$ was improved when media included 2.5 mM sodium citrate to complex iron, reaching a density of 2.76 x 10^7 cells/mL (Fig. 1A). Attempts to culture *Sideroxydans* sp. CL21 on 5 mM sodium citrate alone showed no growth beyond that of a no-substrate control (Fig. 1A), demonstrating *Sideroxydans* sp. CL21 cannot conserve energy from citrate. As Fe(II) was the only available electron donor, these results confirm that *Sideroxydans* sp. CL21 can grow as a lithoautotrophic iron oxidizer.

Sideroxydans sp. CL21 was cultured on commercial and biogenic magnetite to assess its growth on solid iron minerals. Cells grew better on the biogenic versus commercial magnetite (Fig. 1B). This may be due to the lower crystallinity and higher solubility of biogenic magnetite, which sheds more Fe(II) into solution than commercial magnetite (25). The biogenic magnetite, which was produced from ferrihydrite by the iron-reducer *Shewanella*, may also contain extracellular metabolites that could enhance iron oxidation activity and growth in *Sideroxydans* sp. CL21 (26).

Sideroxydans sp. CL21 was also tested for growth on sulfur substrates. The genome includes *dsrAB* genes that encode a reverse dissimilatory sulfite reductase (rDSR) (19). It has previously been cultured on FeS and in agarose-stabilized media in gradient tubes with either thiosulfate or thiosulfate plus H_2 or lactate (18). Since agarose may provide a source of C (27, 28), we used liquid media without an organic carbon source to confirm whether cells could grow using individual sulfur substates as their sole electron donor. In these experiments *Sideroxydans* sp. CL21 grew on thiosulfate and elemental sulfur (Fig. 1B), reaching densities near 10^7 cells/mL. However, growth was slower (18-19 days) and cell density was lower than that of Fe(II)-grown cells (Fig. 1A, 1B). Nonetheless, this shows *Sideroxydans* sp. CL21 is capable of two additional lithoautotrophic metabolisms using thiosulfate and S(0) as electron donors.

Previous studies showed growth of *Sideroxydans* sp. CL21 in multi-substrate experiments where lactate was combined with inorganic substrates (FeS, Fe(0), H_2, NaS_2O_3) in agarose gradient tubes (18), yet cells were never successfully grown on lactate alone. Our data show that *Sideroxydans* sp. CL21 grew in liquid culture with either 5 mM lactate (Fig. 1C, 2A) or 5 mM pyruvate (Fig. 1D, 2B) as the sole electron donor. Cells cultured on lactate grew to an order of magnitude higher density than those cultured on Fe(II), reaching 4.8 x 10^8 cells/mL in 14 days (Fig. 1C). Together, these results show *Sideroxydans* sp. CL21 can grow organotrophically, and likely organoheterotrophically, on lactate or pyruvate.

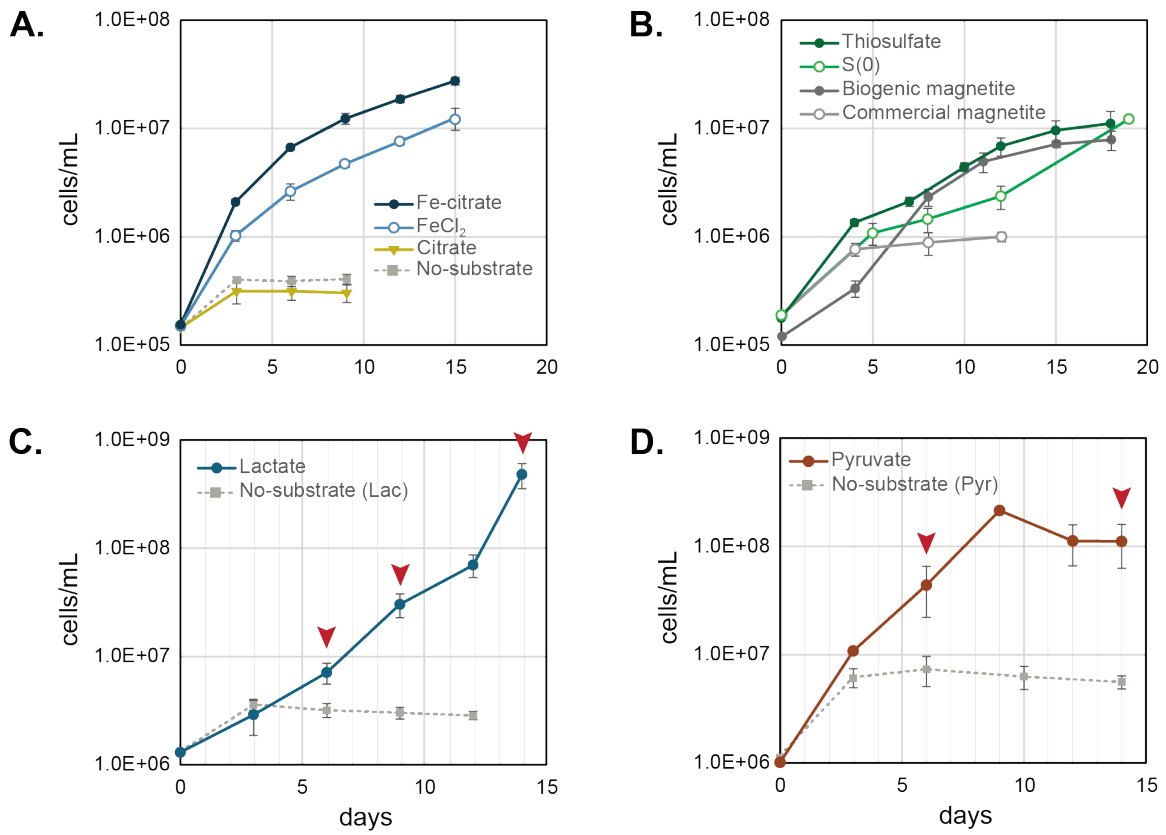

144 **FIG 1.** Growth of *Sideroxydans* sp. CL21 on: (A) $FeCl_2$, $FeCl_2$ + citrate, and citrate compared to
145 a no substrate control; (B) thiosulfate, S(0), biogenic and commercial magnetite; (C) lactate, and
146 (D) pyruvate. Red arrows in panels C indicate days cells were sampled for the Fe(II) spike
147 experiments and transcriptome sequencing. Red arrows in panel D indicate days cells were
148 sampled for Fe(II) spike experiments. Error bars represent one standard deviation between three
149 replicates.

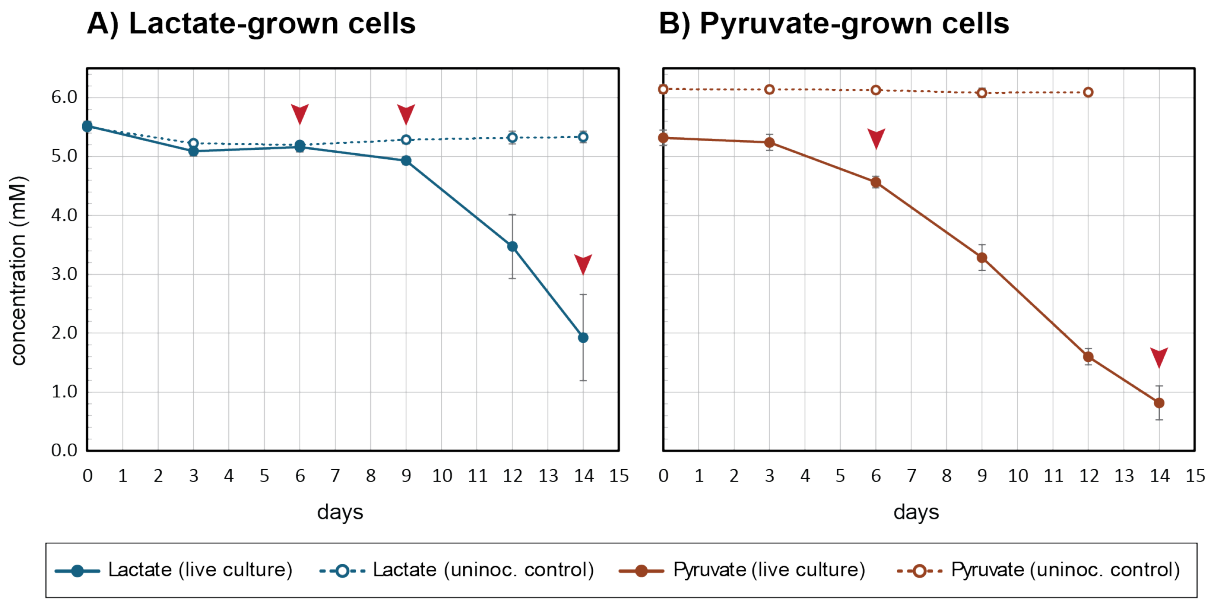

FIG 2. Consumption of (A) lactate and (B) pyruvate over time by live *Sideroxydans* sp. CL21 in growth experiments (Fig. 1C, 1D) versus uninoculated controls. Arrows indicate sampling points for short-term iron oxidation assays (Fig 3). Error bars represent one standard deviation between three replicates.

The potential for mixotrophic energy metabolism

Sideroxydans sp. CL21 cells have the genomic potential to carry out multiple energy metabolisms simultaneously (mixotrophy), but this requires further experimental proof. Our approach was to determine whether *Sideroxydans* sp. CL21 cells grown on short chain organic acids could also oxidize ferrous iron in a short-term assay. We first harvested lactate-grown cells on days 6, 9, and 14 then added a 400 µM "spike" of $FeCl_2$, and measured Fe^{2+} concentration over time. On Day 6, live cells (7.1 x 10^6 cells/mL) did not oxidize iron within the 60-minute experiment. On Day 9 (3.3 x 10^7 cells/mL), the modest amount of iron oxidation was mostly driven by a single bottle, 6A, which had a higher cell density than the other replicates, making it closer to late-log phase (Fig. 3A, Fig. S1). In contrast, with live cells (4.8 x 10^8 cells/mL) harvested on Day 14, iron was completely oxidized within 15 minutes (Fig. 3A) despite the presence of >1 mM of lactate remaining in the cultures (Fig. 2A). This difference in response between mid- and late-log cultures indicates iron oxidation in *Sideroxydans* sp. CL21 is regulated. We also tested pyruvate-grown cells (Fig. 1D, 2B) and found *Sideroxydans* sp. CL21 was primed to oxidize iron on both Day 6 (4.4 x 10^7 cells/mL) and Day 14 (1.1 x 10^8 cells/mL) (Fig. 3B). Together, these results demonstrate that *Sideroxydans* sp. CL21 has the ability to oxidize iron while growing on organic acids, indicating that cells are capable of mixotrophic energy metabolism. Furthermore, because iron oxidation is regulated, we are able to use these samples to investigate gene expression differences between iron-oxidizing and non-iron-oxidizing conditions.

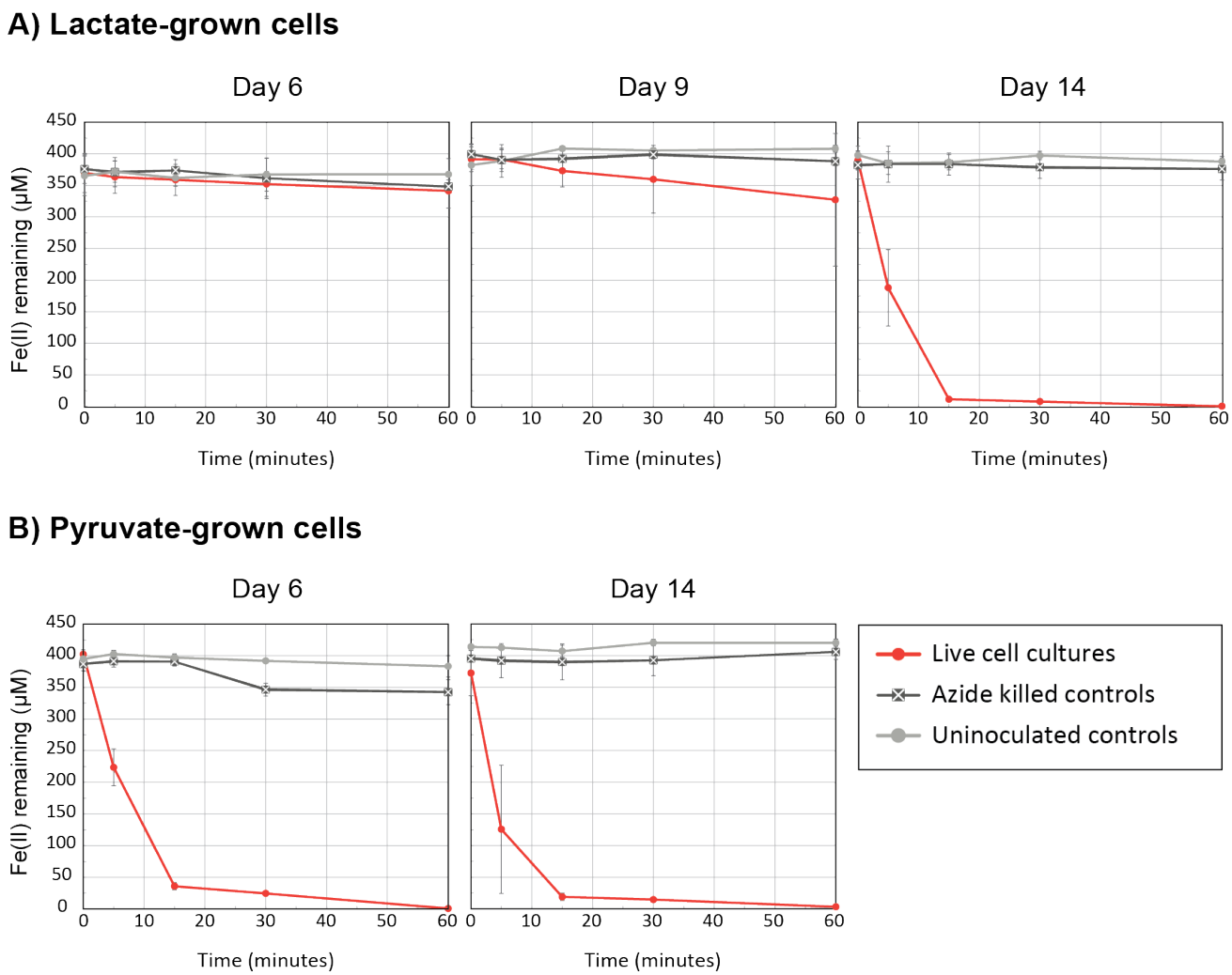

FIG 3. Results of Fe(II) spike assays for lactate- and pyruvate-grown cells. Aliquots of live, lactate-grown *Sideroxydans* sp. CL21 from the transcriptome experiment (Fig. 1C, 2A) rapidly oxidized iron on Day 14 compared to Day 6 or Day 9 (A). Cells from pyruvate growth experiments (Fig. 1D, 2B) rapidly oxidized iron on both Day 6 and Day 14 (B). Error bars represent one standard deviation between three replicates.

Transcriptomics

Lactate-grown cultures were harvested for transcriptomics after aliquots were taken for the Fe(II)-spike experiments on Days 6, 9, and 14 (Fig. 1C, 2A). We present the transcriptome data as Z-scores, calculated from the normalized, regularized log (rlog) transformed read data. This gives a measure of a gene's expression on a log scale relative to the mean expression (Z-score = 0) of all genes at a given time point.

185 ## Expression of lactate and carbon fixation genes

186 The *Sideroxydans* sp. CL21 genome contains six genes for lactate oxidation. These genes
187 are co-located in the genome and encode a lactate response regulator (LldR), L-lactate
188 dehydrogenase (LldE), L-lactate dehydrogenase (LldG), L-lactate dehydrogenase (LldF), D-
189 lactate dehydrogenase (Dld), and lactate permease (LldP) (Fig. 4A). The genes *lldR*, *dld*, and
190 *lldP* set *Sideroxydans* sp. CL21 apart from other closely related Gallionellaceae isolates *S.*
191 *lithotrophicus ES-1* and *S. emersonii* MIZ01 that are unable to oxidize lactate (Fig. 4A). As
192 expected, all six of the *Sideroxydans* sp. CL21 lactate oxidation genes were consistently
193 expressed throughout the experiment (Fig. 4B, Table S1). None of the genes were significantly
194 up- or down-regulated between the timepoints (Fig. 4B, Table S1), which fits with the consistent
195 availability of lactate in the media (Fig. 2A).

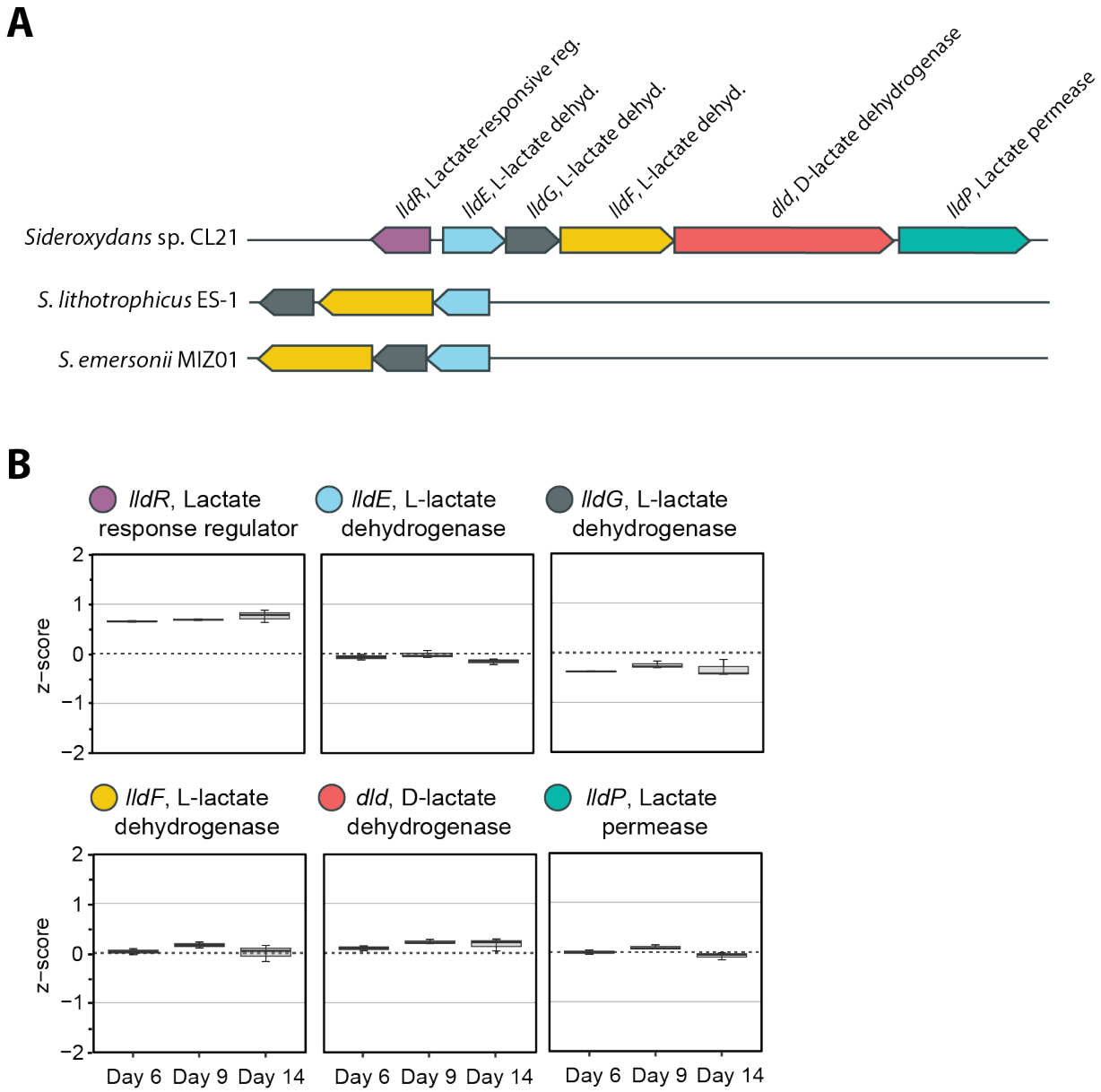

FIG 4. A) The six lactate oxidation genes encoded by *Sideroxydans* sp. CL21 and B) their patterns of expression on days 6, 9, and 14. Expression is represented by Z-score, which shows the expression of each gene relative to the mean gene expression (0) at the time point. Error bars represent the spread of the interquartile range.

When cultured with solely inorganic substrates, *Sideroxydans* sp. CL21 grows lithoautotrophically fixing CO_2 via ribulose bisphosphate carboxylase (RuBisCo) and the Calvin–Benson–Bassham (CBB) cycle (26). High concentrations of organic carbon might be expected to promote heterotrophy and suppress autotrophy, yet lactate-grown *Sideroxydans* sp. CL21 still expressed genes for both Form I and Form II RuBisCo at all timepoints (Fig. S1B). Expression of Form I RuBisCo was relatively low while expression of Form II RuBisCo was

207 high and greater than mean total expression at all three timepoints (Fig. S1B, Table S1). Form II
208 RuBisCo has a higher affinity for oxygen (29), so its higher expression relative to Form I would
209 be consistent with the micro-oxic culturing conditions used in our experiments. While further
210 metabolic evidence is needed, high expression of the gene encoding Form II RuBisCo suggests
211 *Sideroxydans* sp. CL21 could continue to fix CO_2 while oxidizing lactate.

212 Expression of iron oxidation genes

213 The different iron oxidation activities of lactate cultures prompted us to investigate
214 whether this ability corresponds to expression of iron oxidation genes. *Sideroxydans* sp. CL21
215 has multiple iron oxidase genes, three copies of *cyc2* and two copies of *mtoA*. Though there was
216 variation in expression between the copies, overall both *cyc2* and *mtoA* were highly expressed on
217 all three days (Fig. 5A, 5B). Compared to Day 6 (no iron oxidation), expression of *cyc2* or *mtoA*
218 genes was not significantly up- or down-regulated on Day 14, when iron oxidation was rapid
219 (Fig. 5A, 5B, Table S1). Thus, expression of known iron oxidase genes did not correspond to
220 cells' ability to oxidize iron.

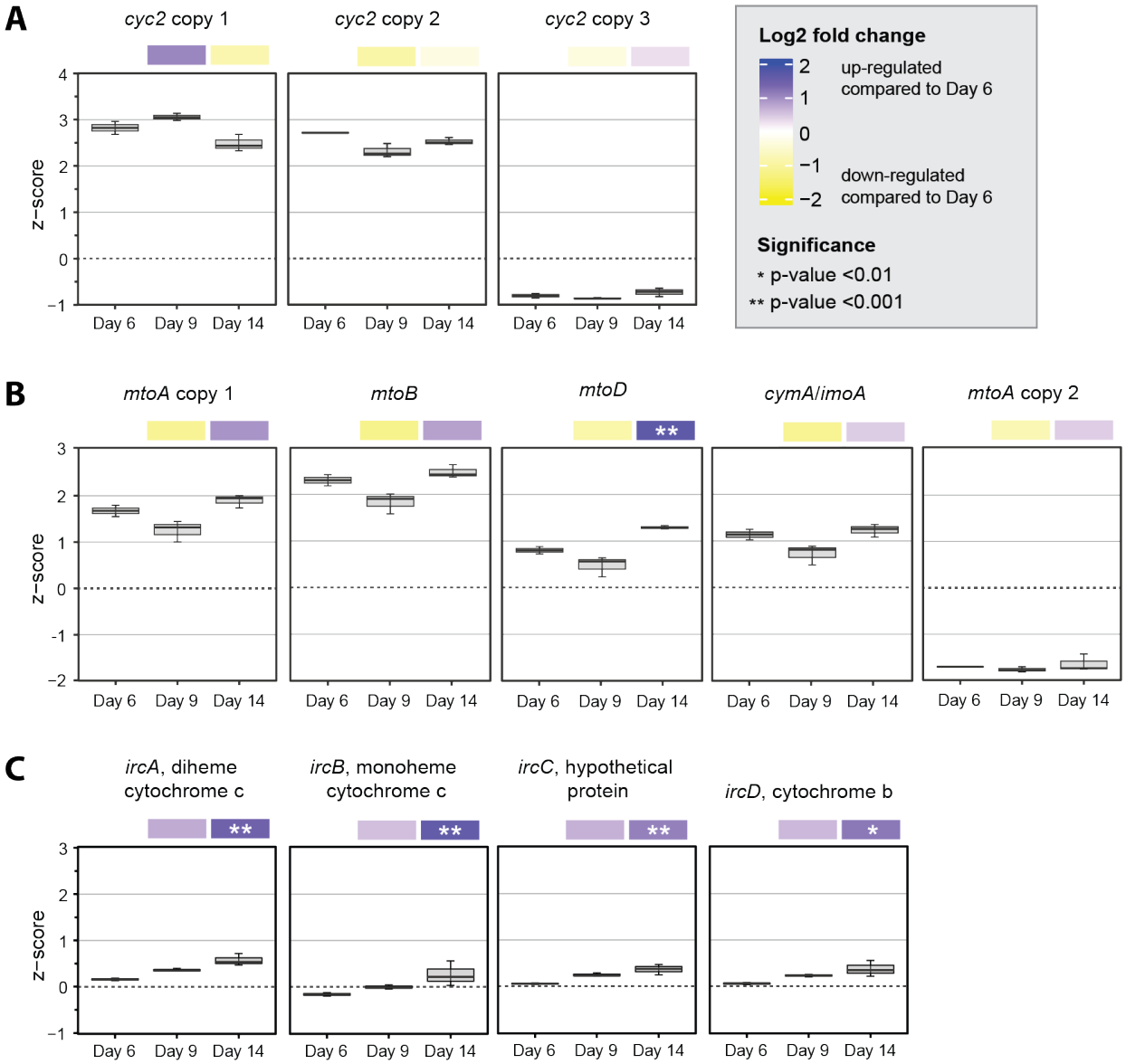

FIG 5. Boxplots of z-score normalized expression for each time point with heatmaps showing the Log2 Fold Change in expression between Day 9 and Day 14 versus Day 6. Expression is represented by Z-score, which shows the expression of each gene relative to the mean gene expression (0) at the time point. Z-score was calculated from rlog normalized count data from DESeqs2. Data is shown for: (A) *cyc2* iron oxidase genes; (B) *mtoA* iron oxidase, *mtoB* porin, and *mtoD*, *imoA/cymA* periplasmic *c*-type cytochrome genes; and (C) *ircABCD* Fe(II)-responsive genes. Error bars represent the spread of the interquartile range.

Both known iron oxidases, Cyc2 and MtoAB, are predicted to be outer membrane, porin-cytochromes, allowing them to oxidize Fe(II) outside the cell. Though functionally unverified, porin-cytochrome c complex 3 (PCC3) is predicted to be an outer membrane porin-cytochrome

232 complex similar to, but larger than, the MtoAB iron oxidase complexes (24). PCC3 is widely
233 distributed among various FeOB genomes (19, 24), making PCC3 another potential iron
234 oxidation mechanism. *Sideroxydans* sp. CL21 has two copies of the PCC3 gene cluster. Each
235 consists of four genes predicted to encode an extracellular multiheme cytochrome c (MHC), a
236 porin, a periplasmic MHC, and an inner membrane protein. Analysis of the Z-scores, where
237 mean expression is 0, showed both copies of PCC3 were expressed higher than the mean (Z-
238 score ~1; Fig. S1), yet not as highly as *cyc2* or *mtoA* (Z-score ~3; Fig. 5A, 5B, Fig. S1) across all
239 three time points. From Day 6 to Day 14, PCC3 copy 1 was downregulated while PCC3 copy 2
240 was upregulated, though the only significant (p-value <0.01) change was to the inner membrane
241 protein of PCC3 copy 2 (Fig. 6, Fig. S1, Table S1).

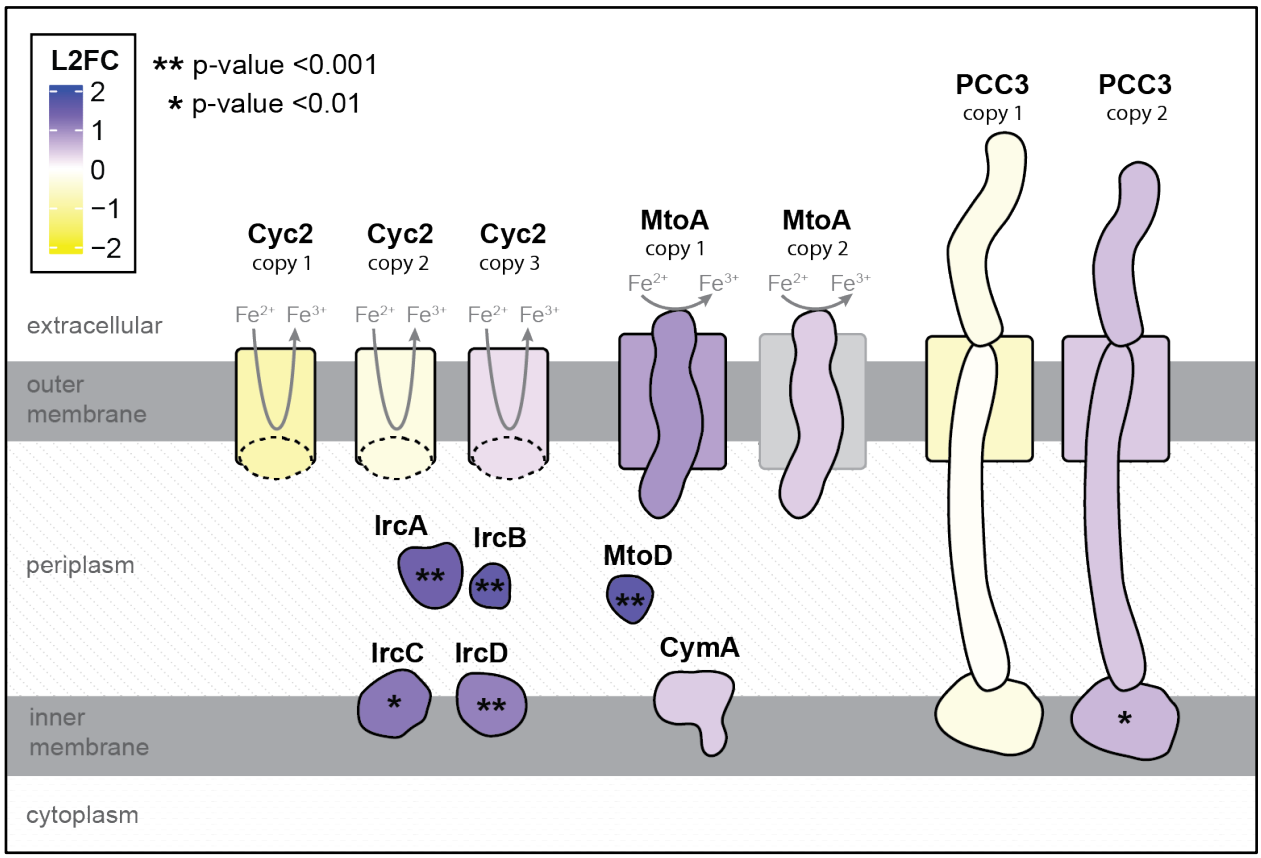

242 **FIG 6.** Cartoon schematic of iron oxidases, outer membrane cytochrome, porin, periplasmic, and
243 inner membrane proteins colored by log2 fold change (L2FC) in normalized, rlog transformed
244 gene expression between Day 14 and Day 6. Positive numbers (blue) were upregulated on Day
245 14 relative to Day 6. Asterisks indicate the gene encoding a particular protein was significantly
246 upregulated.

247 Iron oxidases are just one part of FeOB extracellular electron transport pathways, which
248 require additional cytochromes to convey electrons to the terminal oxidase or quinone pool.
249 *Sideroxydans* sp. CL21 has genes encoding two *c*-type cytochromes, the monoheme MtoD and
250 tetraheme CymA/ImoA, co-located in the genome next to *mtoA* copy 1. Based on genomic

251 context and previous genetic/biochemical characterization, these proteins may form part of the
252 Mto iron oxidation pathway, moving electrons from the MtoA iron oxidase to the electron
253 acceptor and/or quinone pool (30–33). Here, *mtoD* and *cymA/imoA* were upregulated at late log
254 (Day 14) relative to Day 6, with *mtoD* being significantly upregulated (p-value <0.001) (Fig. 5,
255 Fig. 6). In this case, the iron oxidation capability corresponds best with expression of the
256 periplasmic electron carrier gene *mtoD*.
257 *Sideroxydans* sp. CL21 also has homologs to the four "Fe(II)-responsive" genes
258 identified in *S. lithotrophicus* ES-1 (Slit_1321-Slit_1324 (Zhou et al. 2021)). We refer to these
259 genes as "*ircABCD"* for "**i**ron **r**esponsive **c**luster." The *irc* genes encode two *c*-type
260 cytochromes, diheme (IrcA) and a monoheme (IrcB), both predicted to be periplasmic. They also
261 encode a hypothetical protein (IrcC) and a *b*-type cytochrome (IrcD), with predicted localization
262 in the inner membrane (Fig. 6). These genes were upregulated when *S. lithotrophicus* ES-1 was
263 grown on Fe(II) versus thiosulfate (10) and also highly expressed in *Sideroxydans* sp. CL21
264 when grown with Fe(0) (26). In our lactate experiment, expression of these genes increased as
265 cells approached late-log phase (Day 14) and all were significantly upregulated on Day 14
266 relative to Day 6 (Fig. 5C, Fig. 6). This significant upregulation corresponds to cells' ability to
267 oxidize iron on Day 14.
268 Overall, *Sideroxydans* sp. CL21 seems to be concurrently expressing genes for its known
269 and putative iron oxidases (*cyc2*, *mtoA*, and PCC3) regardless of whether cells are capable of
270 iron oxidation. However, expression of genes for periplasmic and inner membrane proteins
271 (*mtoD*, *ircABCD*, inner membrane component of PCC3 copy 2) varies. These genes were
272 significantly upregulated in cells that showed iron oxidation activity, making them potential
273 markers of iron oxidation activity.

274 Discussion

275 In this study, we demonstrated that *Gallionellaceae Sideroxydans* sp. CL21 exhibits
276 remarkable metabolic versatility. *Sideroxydans* sp. CL21 can utilize a wide range of substrates,
277 including short-chain organic acids such as lactate and pyruvate, as well as oxidize various
278 soluble inorganic substrates, such as Fe(II) and thiosulfate. Additionally, it can metabolize
279 mineral substrates, including magnetite and elemental sulfur (S(0)). Overall, our findings show
280 that *Sideroxydans* sp. CL21 is capable of organotrophy and lithoautotrophy, with the potential
281 for mixotrophy and organoheterotrophy. This metabolic flexibility likely enhances its
282 competitiveness, and enables it to contribute to a wide range of biogeochemical transformations.
283 Understanding the ecophysiology and biogeochemical roles of facultative iron oxidizers like
284 *Sideroxydans* sp. CL21 requires more than just detecting their presence in environmental
285 samples. We need a means to decipher whether these FeOB are actively oxidizing iron.
286 Developing methods to directly track microbial iron oxidation activity requires (1) the
287 identification of genes encoding the iron oxidation pathway and (2) determining which of these
288 genes can serve as reliable markers of microbial iron-oxidizing activity.

To be a marker of activity, a gene needs to increase in expression with iron oxidation and have minimal to no expression when cells are unable to oxidize iron. Validating marker genes requires study of facultative FeOB, of which there are few in culture, and there ideally needs to be a condition under which cells *cannot* oxidize iron. Previous studies on *S. lithotrophicus* ES-1 showed differential gene expression of cells grown on Fe(II)-citrate and thiosulfate, but thiosulfate-grown cells were able to oxidize iron quickly with no lag after the substrate was switched to Fe(II). In contrast, *Sideroxydans* sp. CL21 grown on lactate was surprisingly unable to oxidize iron until late-log phase (Day 14), giving an opportunity to compare gene expression of iron-oxidizing and non-iron-oxidizing conditions.

Relationship between iron oxidation gene expression and activity

Although significant progress has been made in assigning function to the key iron oxidases such as Cyc2 and MtoA (10, 20, 33–35), the pathway is likely more complex, and additional iron oxidases may yet be discovered. Genes encoding the larger multiheme cytochrome complexes PCC3_1 and PCC3_2 are expressed at higher than mean levels. PCC3s are predicted to be large outer membrane cytochrome (OMC)-porin complexes (Fig. 6) (24), and while their function has not been tested, as OMCs, they could in principle oxidize iron. Thus, based on the *Sideroxydans* sp. CL21 transcriptome, there are at least four possible iron oxidases (Cyc2, MtoA, and the PCC3_1 and PCC3_2 cytochromes) with various proteins that could direct electrons to terminal oxidases or reverse electron transport pathways.

One might expect the expression of iron oxidase genes to correlate with iron oxidation, but our results show that the well-characterized iron oxidase genes *cyc2* and *mtoA* are always highly expressed in our experiments, and thus do not correspond to iron oxidation ability. This differs from *S. lithotrophicus* ES-1, which has very low expression of *mtoA* on dissolved Fe^{2+} but upregulates *mtoA* when grown on solid Fe(II)-containing minerals smectite and magnetite (10, 22, 23) . We showed that *Sideroxydans* sp. CL21 grows on magnetite, and though magnetite was not present in lactate-grown cultures, expression of *mtoA* may still indicate a readiness to take up electrons from solid minerals. *Sideroxydans* sp. CL21 is more like *S. lithotrophicus* ES-1 in its high expression of *cyc2*. In *S. lithotrophicus* ES-1, expression of *cyc2* (one of three copies) is high even when cells are cultured on thiosulfate (10). Similarly, *Sideroxydans* sp. CL21 highly expresses two of its three *cyc2* copies when grown on lactate. Expression of *cyc2* is also generally high in marine iron-oxidizing Zetaproteobacteria (20). However, *S. lithotrophicus* ES-1 additional copies of *cyc2* are iron-responsive (10). In theory, Cyc2 production could be post-transcriptionally regulated. However, this is not the case in *S. lithotrophicus* ES-1, since proteome data shows Cyc2 is highly expressed on Fe(II) (dissolved Fe^{2+} and magnetite (23)) and thiosulfate (25). One explanation for the overall high expression is that these FeOB maintain readiness or, in the case of *Sideroxydans* sp. CL21, partial readiness to oxidize iron. In any case, because *cyc2* expression does not correspond to iron oxidation activity, *cyc2* (alone) is not an accurate indicator of biotic iron oxidation.

327 Beyond iron oxidases, iron oxidation activity also requires electron carrier proteins in the
328 periplasm and inner membrane. Currently, there is limited evidence supporting other essential
329 components of the pathway, particularly periplasmic electron carriers and inner membrane
330 proteins (Table S3). Our findings contribute to filling this gap by providing evidence for the
331 involvement of genes encoding predicted periplasmic and inner membrane proteins. In fact, the
332 genes that were most upregulated in cells that showed iron oxidation (Day 14) were periplasmic
333 *c*-type cytochrome genes *ircA*, *ircB*, and *mtoD* (Fig. 6), followed by the inner membrane protein
334 genes *ircC*, *ircD*, and the PCC3_2 inner membrane component. There is accumulating evidence
335 for the involvement of *irc* genes in iron oxidation. Homologs are widespread among
336 Gallionellaceae and found in several other FeOB including *Leptothrix cholodnii* SP-6,
337 *Rhodoferax* spp., and several Zetaproteobacteria (Table S2; (19, 21)). In *S. lithotrophicus* ES-1,
338 *irc* genes are upregulated on iron-oxidizing cultures versus thiosulfate-oxidizing ones (10). The
339 periplasmic di- and mono-heme *c*-type cytochrome genes (*ircA* and *ircB*) are homologs of *grcJ*
340 and *grcI* in *Ghiorsea bivoria* TAG-1. In *G. bivoria* TAG-1, GrcJ is significantly upregulated
341 under iron-oxidizing vs. H_2-oxidizing conditions and expression of *grcJ* increases over time
342 when cells were grown with Fe(II) (21). In lactate-grown *Sideroxydans* sp. CL21, upregulated
343 expression of *ircABCD* corresponded to the cells' potential to oxidize iron in late-log cultures
344 (Day 14). Thus, it appears that cells increase expression of electron carrier genes like *irc*, *grc*,
345 and *mtoD* when cells are ready to oxidize iron, making them the best candidates thus far for
346 markers of iron oxidation potential.
347 The results to date suggest that the iron oxidation pathway is not regulated as a complete
348 set in the neutrophilic FeOB Gallionellaceae. Instead, at least one OMC (one Cyc2) is
349 constitutively expressed, which could serve multiple purposes. Cyc2 may operate as an Fe(II)
350 sensor to tell the cell when it is time to increase expression of the iron oxidation pathway. An
351 issue with this pathway is that OMCs are complicated to produce; they must be secreted to the
352 periplasm, where the heme cofactor is attached and then inserted into the outer membrane with
353 proper folding. Each of these three steps involves separate machinery, so this requires substantial
354 space in the inner membrane and periplasm, which may interfere with the electron transfer
355 pathway. Thus, expressing Cyc2 and other OMCs ahead of iron oxidation may be a strategy for a
356 quicker iron oxidation response. In contrast to the OMC, many of the periplasmic and inner
357 membrane components are smaller and would be easier to produce when they are required. This
358 strategy also allows the organism to express different periplasmic and inner membrane proteins
359 to match different iron substrates (Fe(II), magnetite, chelated Fe(II)), which have varied redox
360 potentials (36, 37), as is the case in *Geobacter* (38).
361 Thus, we conclude that the Gallionellaceae may implement a multistage production of the
362 iron oxidation pathway, with a subset of the OMCs expressed proactively, followed by additional
363 OMCs and the rest of the pathway once iron oxidation is required. This may be further tested as
364 additional facultative FeOB are isolated. In the meantime, we will need to carefully parse the
365 expression profiles to interpret FeOB activity in the environment, though the *irc*/*grc* genes are
366 promising markers.

C utilization among FeOB

Sideroxydans sp. CL21 is distinct among the current Gallionellaceae isolates in its ability to grow on organic acids. However, other uncultured mixotrophic or organo(hetero)trophic FeOB are likely present in C-rich environments. A pangenomic analysis of *Gallionellaceae* isolates and environmental MAGs reveals that the potential for lactate utilization is rare but not unique, as it has been observed in some genomes from the Crystal Bog humic lake (Wisconsin) and freshwater lakes near Kuujjuarapik-Whapmagoostui (Canada) (19, 39–41). Active organic substrate utilization by FeOB fundamentally alters their role in the carbon cycle. While FeOB are traditionally considered autotrophs that fix CO_2, the ability to grow organotrophically suggests they may also contribute to the degradation of organic carbon in situ. The ability to grow on organics may provide a significant ecological advantage in specific habitats, especially wetlands and peatlands. In peatlands, mixotrophic FeOB face competition with both aerobic and anaerobic microorganisms for organic intermediates such as lactate and pyruvate. However, FeOB exhibit a unique advantage by coupling the consumption of these substrates to aerobic respiration under microaerophilic conditions. This metabolic flexibility of FeOB enables them to thrive in environments like peatlands, where fluctuating water tables create dynamic oxic-anoxic gradients, offering transient microaerophilic niches. Thus, such versatility may be key to their survival and dominance in specific ecosystems, and play integral roles in biogeochemical iron and C cycling in dynamic environments.

Implications of FeOB organotrophy for wetland C cycling

By demonstrating the versatility of FeOB metabolism and its genetic basis, our findings provide a foundation for understanding the broader biogeochemical roles of FeOB in wetland ecosystems and how they connect iron and C cycles. It is already recognized that organotrophic iron-reducing bacteria can compete for organic carbon, thus shunting carbon away from methanotrophs, which could reduce wetland methane emissions (42–46). FeOB help promote this process by replenishing the supply of Fe(III). If the FeOB are autotrophic, then iron oxidation drives the regeneration of organic C, partly reversing the effect of organotrophic iron reduction and muting the effects on methanogenesis. But if the FeOB are organotrophic, they would join the competition for organics and, if sufficiently abundant and active, contribute to the suppression of methanogenesis. These are theoretical effects; evaluating the actual effects of FeOB organotrophy requires specifically monitoring FeOB C metabolism in the wetland environment and soil incubations. The potential iron oxidation gene markers would give us a way to link iron oxidation activity to organotrophic metabolisms via genome-resolved metatranscriptomics, paving the way toward deeper insights into FeOB influences on wetland biogeochemistry and interactions with wetland communities. This knowledge is essential for predicting how iron and C cycling—and associated greenhouse gas fluxes—will respond to environmental changes.

Methods

Growth experiments

For all growth experiments, *Sideroxydans* sp. CL21 was cultured in triplicate, in 150 mL serum bottles with 80 mL of modified Wolfe's minimal medium (MWMM; containing 1.0 g NH_4Cl, 0.5 g $MgSO_4 \cdot 7H2O$, 0.2 g $CaCl_2$, and 0.05 g K_2HPO_4 per liter). All cultures were amended with a 0.1% vol/vol addition each of ATCC trace vitamins and trace minerals. To keep micromolar concentrations of oxygen, headspaces were flushed daily with low-oxygen gas mix (2% O_2, 20% CO_2, 76% N_2). A Firesting oxygen spot sensor (Pyro Science) was used to measure and monitor oxygen concentrations. With the exception of lactate and pyruvate cultures, all bottles were incubated on their sides in a dark culturing cabinet at room temperature. Lactate and pyruvate bottles were incubated upright in a New Brunswick Innova 42 shaking incubator at 20°C, 75 RPM. Growth for all cultures was measured by direct cell counting whereby cells were stained with Syto-13 then counted manually in a Petroff-Hauser counting chamber under fluorescence microscopy.

Lactate cultures included a one-time addition of sodium DL-lactate (CAS 72-17-3) for a concentration of 5 mM and were buffered with 10mM of 2-(N-morpholino)ethanesulfonic acid (MES) at pH 6.0. Likewise, citrate (CAS 6132-04-3), pyruvate (CAS 113-24-6), thiosulfate (CAS 10102-17-7), and S(0) cultures were buffered with MES at pH 6.0 and given a one-time dose of sodium citrate dihydrate, sodium pyruvate, sodium thiosulfate pentahydrate, or elemental sulfur powder for a starting concentration of 5 mM. Biogenic and commercial magnetite cultures were each given a single addition of magnetite (1 g/L). Biogenic magnetite was synthesized by incubating *Shewanella oneidensis* MR-1 in Luria-Bertani (LB) media with two-line ferrihydrite for 10-12 days in an anerobic chamber. After incubation a magnet was used to hold the magnetite in place while the supernatant was decanted. Minerals were washed 3x with deoxygenated water, then dried in an anaerobic desiccator.

$FeCl_2$ cultures were buffered with 50 mM of MES at pH 6.0. These cultures were given a daily addition of $FeCl_2$ ranging from 250 µM on Day 0 to 500 µM on Day 14. The $FeCl_2$ + citrate experiment was conducted under these same conditions plus a one-time addition of 2.5 mM sodium citrate.

Organic acids measurements

Samples from lactate and pyruvate cultures were collected, filtered with a 0.22 µm syringe filter, and stored at 4°C. Concentration of organic acids (lactate, pyruvate, formate, acetate) were measured by high-performance liquid chromatography (HPLC). Measurements were made on a Shimadzu HPLC with a Photodiode Array Detector (model MPD-40) with a Alltech Prevail Organic Acid 5 µm 150 x 4.6 mM column and guard column. Organic acids were eluted at room temperature with 25 mM KH_2PO_4 at pH 2.5, adjusted with phosphoric acid, at 1

440 mL/minute. Absorbance was read at 210 nm to quantify compounds based on peak area.
441 Instrument control and data collection were performed using LabSolutions software (v. 5.106
442 SP1). Peak areas were exported to Microsoft Excel where calibration curves were generated by
443 linear regression of authentic standard peak areas and used to calculate concentrations.

444 Transcriptome experiment

445 *Sideroxydans sp.* CL21 was cultured in 5 mM lactate as described above. Bottles were
446 inoculated with stationary phase, lactate-adapted cells. Cell counts and lactate measurements
447 were taken on days 0, 3, 6, 9, 14. On days 6, 9, and 14, aliquots of cultures were used in Fe(II)
448 spike assays (described below) and bottles were sacrificed in biological sextuplets for
449 transcriptome sequencing. For all sacrifices, a 1:10 vol/vol of stop solution (buffer-saturated
450 phenol:absolute ethanol at a 1:9 vol/vol) was injected into the bottles to stop transcription. Cells
451 were then harvested by filtering onto a 0.22 µm polyethersulfone (PES) filter and stored at -80°C
452 until RNA extraction.

453 Fe(II) spike assay

454 Fe(II) spike assays were performed at different timepoints to test *Sideroxydans* sp.
455 CL21's response to Fe(II) when grown on lactate and pyruvate. For these assays, 10 mL of
456 culture were extracted from each of the six inoculated serum bottles. Of this, 5 mL was incubated
457 in 5 mM sodium azide for 20 minutes to create the azide-killed control. The other 5 mL was
458 untreated and served as the "live cell" samples. A 5 mL aliquot was taken from six uninoculated
459 bottles for the uninoculated control. All samples were bubbled with a 2% O_2, 20% CO_2, 78% N_2
460 gas mix throughout the experiment to keep oxygen levels consistent and low. Each sample, live
461 and control, was spiked with 20 µL of 100 mM $FeCl_2$ for a 400 µM starting concentration.
462 Samples were collected at 0, 5, 15, 30, and 60 minutes and preserved in a 1:1 mix with 40 mM
463 sulfamic acid. After all samples were collected, a spectrophotometric ferrozine assay was used to
464 measure ferrous iron concentrations (47, 48).

465 RNA extraction and sequencing

466 RNA was extracted from cells collected on PES filters using a RNeasy PowerSoil RNA
467 kit (Qiagen). Extracted RNA was treated with three RNase inhibitors (1 µL Invitrogen
468 SUPERase, 3 µL RNaseOUT, 1.25 µL Ambion RNase Inhibitor) to prevent degradation. Total
469 RNA was quantified using a Qubit RNA HS assay kit from Invitrogen and quality was assessed
470 with an Agilent fragment analyzer. A Zymo RNA Clean & Concentrator™-5 kit was used to
471 remove excess salts and DNA from all samples. After clean-up, three samples with the best yield
472 and quality from each timepoint (Day 6 - 12.6, 13.2, 29.6 ng/µL; Day 9 – 34.6, 43.0, 25.6 ng/µL;
473 Day 14 – 82.0, 20.0, 92.0 ng/µL), along with sample 6A from Day 9 (33.4 ng/µL) were selected
474 for sequencing. Ribosomal RNA depletion and library preparation were done using a Zymo-Seq

475 RiboFree® Total RNA Library Kit. Sixty-four ng of total RNA from each samples was
476 sequenced on an Illumina NextSeq 2000 using a P2 100-cycle protocol yielding up to 40 GB of
477 data (up to 400 million single-end reads). All clean-up, library prep and sequencing was
478 performed by the University of Delaware DNA Sequencing & Genotyping Center.

479 Transcriptome QC and analysis

480 Raw transcriptome reads were quality checked using FastQC v0.11.9 (49). Reads were
481 trimmed and adaptor sequences were removed using TrimGalore! v.0.6.6 (50) and Cutadapt v4.4
482 (51). A minimum quality score of 28 and minimum length of 75 bp were applied to filter out
483 poor reads. Post-trim, the read quality was reassessed with FastQC v0.11.9 (49) and SortMeRNA
484 v4.3.6 (52) was run on all samples to remove any rRNA sequences before mapping.
485 Reads were mapped to the closed, RefSeq annotated genome of *Sideroxydans* sp. CL21
486 (GCF_902459525.1) using Bowtie 2 v2.5.1 (53) and Samtools v1.10 (54). The average
487 alignment rate per sample was 97%, with the exception of Day 6, Sample 3B which was 73%.
488 Read counts were reported using Htseq v2.0.2 (55). After comparing the total number of reads
489 mapped for each sample and the overall alignment rates, we determined that Day 6, Sample 3B
490 was an outlier with potential contamination and too few quality reads to be useful. To be
491 thorough, we ran and compared the DGE analysis (described below) with and without Day 6
492 Sample 3B. Exclusion of Day 6 Sample 3B did not affect the overall findings or change whether
493 the differential expression of our genes of interest was significant. Instead, removing the outlier
494 decreased noise and made the dataset more precise.
495 Differential gene expression was analyzed in R v4.4.0 (56) with RStudio v2023.06.0
496 Build 421 (57) using the DESeq2 v1.26.0 (58) package. Data was normalized using DESeqs
497 default algorithm which uses an estimation of size factors to control for differences in
498 sequencing depth. P-values were determined with the Wald Test and adjusted for false discovery
499 rate (FDR) using the Benjamini-Hochberg (BH) correction. An alpha of 0.01 was set as the cut-
500 off for significance. Reports of normalized count data for each sample were generated using the
501 regularized logarithm (rlog) transformation (58). This rlog counts data was used to calculate Z-
502 score to analyze the variance of individual genes across samples. To test validity of these
503 transformations, we checked the expression of housekeeping genes for DNA gyrase and RNA
504 polymerase *(gyrA, gyrB*, and *rpoA*). Their even expression over all timepoints indicates the rlog
505 and Z-score transformations were successful (Fig. S1A, Table S1).

506 Identification and analysis of the Fe(II)-responsive (*irc*) gene
507 cluster

508 Homologs of the Fe(II)-responsive (*irc*) gene cluster were identified by using cblaster
509 (59) to search the NCBI database for BLAST hits (e-value cut-off < 1E-10) to the *irc* genes of
510 *Sideroxydans* sp. CL21 that were located within 20,000 bp of each other in their respective

genomes. Positive hits needed to contain at least three of the genes, excluding the Hsp33 chaperone. Results were visualized using clinker (60). PSORTb 3.0 (61), Gneg-mPLoc (62), PredictProtein (63), and InterProScan (64, 65) were used to predict subcellular localization and domains of the *irc* genes.

Data availability

Transcriptomic data were uploaded to NCBI BioProject PRJNA1216980.

Acknowledgements

This work was funded by the National Science Foundation (EAR-1833525 to C.S.C., MCB-1817651 to C.S.C.) and the Office of Naval Research (N00014-17-1-2640 C.S.C.). R.L.H. was also supported by fellowships from University of Delaware Graduate College and the Microbiology Program/Unidel Foundation. Support from the University of Delaware Center for Bioinformatics and Computational Biology Core Facility (RRID:SCR_017696), including the use of the BIOMIX computer cluster, was made possible through funding from Delaware INBRE (NIH P20GM103446), the State of Delaware, and the Delaware Biotechnology Institute. KK was supported by the Collaborative Research Centre Chemical Mediators in Complex Biosystems (SFB 1127 ChemBioSys, Project Number 239748522), which is funded by the Deutsche Forschungsgemeinschaft.

We also thank Thomas Hanson for his help with the HPLC analyses, Christian Sinjari for his assistance culturing *Sideroxydans* sp. CL21 on magnetite, Jessica Keffer for feedback and editing, and Mark Shaw for sample clean-up and sequencing.

We declare no conflict of interest.

Supplementals

Figures

- **Figure S1** – Line graphs of iron oxidation response of individual bottles on A) Day 6, B) Day 9, and C) Day 14.
- **Figure S2** – Boxplot/heatmap of A) housekeeping genes, B) RuBisCo, C) PCC3 copy 1, D) PCC3 copy 2

541 # Tables

542 - **Table S1** – Differential expression, normalized expression, and Z-score data for key genes
543 - **Table S2** – *ircABCD* homologs in FeOB and FeRB
544 - **Table S3** – Table of existing evidence for the involvement of various genes and proteins in
545 iron oxidation and/or extracellular electron transport.

References

1. Borch T, Kretzschmar R, Kappler A, Cappellen PV, Ginder-Vogel M, Voegelin A, Campbell K. 2010. Biogeochemical redox processes and their impact on contaminant dynamics. Environ Sci Technol 44:15–23.

2. Barros MEC, Rawlings DE, Woods DR. 1984. Mixotrophic growth of a *Thiobacillus ferrooxidans* strain. Appl Environ Microbiol 47:593–595.

3. Akob DM, Hallenbeck M, Beulig F, Fabisch M, Küsel K, Keffer JL, Woyke T, Shapiro N, Lapidus A, Klenk H-P, Chan CS. 2020. Mixotrophic iron-oxidizing *Thiomonas* isolates from an acid mine drainage-affected creek. Appl Environ Microbiol 86:e01424-20.

4. Fleming EJ, Woyke T, Donatello RA, Kuypers MMM, Sczyrba A, Littmann S, Emerson D. 2018. Insights into the fundamental physiology of the uncultured Fe-oxidizing bacterium *Leptothrix ochracea*. Appl Environ Microbiol 84:e02239-17.

5. Hallbeck L, Pedersen K. 1991. Autotrophic and mixotrophic growth of *Gallionella ferruginea*. Microbiology, 137:2657–2661.

6. Tothero GK, Hoover RL, Farag IF, Kaplan DI, Weisenhorn P, Emerson D, Chan CS. 2024. *Leptothrix ochracea* genomes reveal potential for mixotrophic growth on Fe(II) and organic carbon. Appl Environ Microbiol 90:e00599-24.

7. Sobolev D, Roden EE. 2004. Characterization of a neutrophilic, chemolithoautotrophic Fe(II)-oxidizing β -Proteobacterium from freshwater wetland sediments. Geomicrobiol J 21:1–10.

8. Eggerichs T, Wiegand M, Neumann K, Opel O, Thronicker O, Szewzyk U. 2020. Growth of iron-oxidizing bacteria *Gallionella ferruginea* and *Leptothrix cholodnii* in oligotrophic environments: Ca, Mg, and C as limiting factors and *G. ferruginea* necromass as C-source. Geomicrobiol J 37:190–199.

9. Emerson D, Moyer C. 1997. Isolation and Characterization of novel iron-oxidizing bacteria that grow at circumneutral pH. Appl Environ Microbiol 63:9.

10. Zhou N, Keffer JL, Polson SW, Chan CS. 2021. Unraveling Fe(II)-oxidizing mechanisms in a facultative Fe(II) oxidizer, *Sideroxydans lithotrophicus* strain ES-1, via culturing, transcriptomics, and reverse transcription-quantitative PCR. Appl Environ Microbiol 88:e01595-21.

11. Kato S, Itoh T, Iino T, Ohkuma M. 2022. *Sideroxyarcus emersonii* gen. nov. sp. nov., a neutrophilic, microaerobic iron- and thiosulfate-oxidizing bacterium isolated from iron-rich wetland sediment. Int J Syst Evol Microbiol 72:005347.

578 12. Garry M, Farasin J, Drevillon L, Quaiser A, Bouchez C, Le Borgne T, Coffinet S, Dufresne
579 A. 2024. *Ferriphaselus amnicola* strain GF-20, a new iron: and thiosulfate-oxidizing
580 bacterium isolated from a hard rock aquifer. FEMS Microbiol Ecol 100:fiae047.

581 13. Lüdecke C, Reiche M, Eusterhues K, Nietzsche S, Küsel K. 2010. Acid-tolerant
582 microaerophilic Fe(II)-oxidizing bacteria promote Fe(III)-accumulation in a fen. Environ
583 Microbiol 12:2814–2825.

584 14. Küsel K, Blöthe M, Schulz D, Reiche M, Drake HL. 2008. Microbial reduction of iron and
585 porewater biogeochemistry in acidic peatlands. Biogeosciences 5:1537-1549.

586 15. Hädrich A, Taillefert M, Akob DM, Cooper RE, Litzba U, Wagner FE, Nietzsche S,
587 Ciobota V, Rösch P, Popp J, Küsel K. 2019. Microbial Fe(II) oxidation by *Sideroxydans*
588 *lithotrophicus* ES-1 in the presence of Schlöppnerbrunnen fen-derived humic acids. FEMS
589 Microbiol Ecol 95:fiz034.

590 16. Kügler S, Cooper RE, Wegner C-E, Mohr JF, Wichard T, Küsel K. 2019. Iron-organic
591 matter complexes accelerate microbial iron cycling in an iron-rich fen. Sci Total Environ
592 646:972–988.

593 17. Cooper RE, Wegner C-E, McAllister SM, Shevchenko O, Chan CS, Küsel K. 2020. Draft
594 genome sequence of *Sideroxydans* sp. strain CL21, an Fe(II)-oxidizing bacterium.
595 Microbiol Resour Announc 9:e01444-19.

596 18. Cooper RE, Finck J, Chan C, Küsel K. 2023. Mixotrophy broadens the ecological niche
597 range of the iron oxidizer *Sideroxydans* sp. CL21 isolated from an iron-rich peatland.
598 FEMS Microbiol Ecol 99:fiac156.

599 19. Hoover RL, Keffer JL, Polson SW, Chan CS. 2023. Gallionellaceae pangenomic analysis
600 reveals insight into phylogeny, metabolic flexibility, and iron oxidation mechanisms.
601 mSystems 8:e00038-23.

602 20. McAllister SM, Polson SW, Butterfield DA, Glazer BT, Sylvan JB, Chan CS. 2020.
603 Validating the Cyc2 Neutrophilic Iron oxidation pathway using meta-omics of
604 *Zetaproteobacteria* iron mats at marine hydrothermal vents. mSystems 5:e00553-19

605 21. Barco RA, Merino N, Lam B, Budnik B, Kaplan M, Wu F, Amend JP, Nealson KH,
606 Emerson D. 2024. Comparative proteomics of a versatile, marine, iron-oxidizing
607 chemolithoautotroph. Environ Microbiol 26:e16632.

608 22. Zhou N, Kupper RJ, Catalano JG, Thompson A, Chan CS. 2022. Biological oxidation of
609 Fe(II)-bearing smectite by microaerophilic iron oxidizer *Sideroxydans lithotrophicus* using
610 dual Mto and Cyc2 iron oxidation pathways. Environ Sci Technol 56:17443-17453.

611 23. Keffer JL, Zhou N, Rushworth DD, Yu Y, Chan CS. 2024. Microbial magnetite oxidation
612 via MtoAB porin-multiheme cytochrome complex in *Sideroxydans lithotrophicus* ES-1.
613 bioRxiv https://doi.org/10.1101/2024.09.20.614158. In press at AEM.

614 24. He S, Barco RA, Emerson D, Roden EE. 2017. Comparative genomic analysis of
615 neutrophilic iron(II) oxidizer genomes for candidate genes in extracellular electron transfer.
616 Front Microbiol 8:1584.

617 25. Zhou N. 2022. The molecular mechanisms and organic effects on microaerophilic Fe(II)
618 oxidation by *Sideroxydans Lithotrophicus* ES-1. Doctoral dissertation, University of
619 Delaware.

620 26. Cooper RE, Wegner C-E, Kügler S, Poulin RX, Ueberschaar N, Wurlitzer JD, Stettin D,
621 Wichard T, Pohnert G, Küsel K. 2020. Iron is not everything: unexpected complex
622 metabolic responses between iron-cycling microorganisms. The ISME Journal 14:2675–
623 2690.

624 27. Ohta Y, Nogi Y, Miyazaki M, Li Z, Hatada Y, Ito S, Horikoshi K. 2004. Enzymatic
625 properties and nucleotide and amino acid sequences of a thermostable β-agarase from the
626 novel marine isolate, JAMB-A94. Biosci Biotechnol Biochem 68:1073–1081.

627 28. Bannikova GE, Lopatin SA, Varlamov VP, Kuznetsov BB, Kozina IV, Miroshnichenko
628 ML, Chernykh NA, Turova TP, Bonch-Osmolovskaya EA. 2008. The thermophilic bacteria
629 hydrolyzing agar: Characterization of thermostable agarase. Appl Biochem Microbiol
630 44:366–371.

631 29. Badger MR, Bek EJ. 2008. Multiple Rubisco forms in proteobacteria: their functional
632 significance in relation to CO_2 acquisition by the CBB cycle. J Exp Bot 59:1525–1541.

633 30. Beckwith CR, Edwards MJ, Lawes M, Shi L, Butt JN, Richardson DJ, Clarke TA. 2015.
634 Characterization of MtoD from *Sideroxydans lithotrophicus*: a cytochrome c electron
635 shuttle used in lithoautotrophic growth. Front Microbiol 6:332.

636 31. Jain A, Kalb MJ, Gralnick JA. 2022. Reconstructing electron transfer components from an
637 Fe(II) oxidizing bacterium. Microbiology 168:001240.

638 32. Jain A, Coelho A, Madjarov J, Paquete CM, Gralnick JA. 2022. Evidence for quinol
639 oxidation activity of ImoA, a novel NapC/NirT family protein from the neutrophilic Fe(II)-
640 oxidizing bacterium *Sideroxydans lithotrophicus* ES-1. mBio 13:e02150-22.

641 33. Liu J, Wang Z, Belchik SM, Edwards MJ, Liu C, Kennedy DW, Merkley ED, Lipton MS,
642 Butt JN, Richardson DJ, Zachara JM, Fredrickson JK, Rosso KM, Shi L. 2012.
643 Identification and Characterization of MtoA: a decaheme c-type cytochrome of the
644 neutrophilic Fe(II)-oxidizing bacterium *Sideroxydans lithotrophicus* ES-1. Front Microbio
645 3:37.

646 34. Keffer JL, McAllister SM, Garber AI, Hallahan BJ, Sutherland MC, Rozovsky S, Chan CS.
647 2021. Iron oxidation by a fused cytochrome-porin common to diverse iron-oxidizing
648 bacteria. mBio 12:e01074-21.

649 35. Kappler A, Bryce C, Mansor M, Lueder U, Byrne JM, Swanner ED. 2021. An evolving
650 view on biogeochemical cycling of iron. Nat Rev Microbiol 19:360–374.

651 36. Huang J, Jones A, Waite TD, Chen Y, Huang X, Rosso KM, Kappler A, Mansor M,
652 Tratnyek PG, Zhang H. 2021. Fe(II) Redox chemistry in the environment. Chem Rev 121:
653 8161-8233.

654 37. Levar CE, Rollefson DR, Bond. 2012. *In* Gescher, J., Kappler, A., (ed), Microbial Metal
655 Respiration: From Geochemistry to Potential Applications. Springer Berlin Heidelberg p29-
656 48.

657 38. Joshi K, Chan CH, Bond DR. 2021. Geobacter sulfurreducens inner membrane cytochrome
658 CbcBA controls electron transfer and growth yield near the energetic limit of respiration.
659 Mol Microbiol 116:1124–1139.

660 39. Rohwer RR, Kirkpatrick M, Garcia SL, Kellom M, McMahon KD, Baker BJ. 2025. Two
661 decades of bacterial ecology and evolution in a freshwater lake. Nat Microbiol 10:246–257.

662 40. Oliver T, Varghese N, Roux S, Schulz F, Huntemann M, Clum A, Foster B, Foster B, Riley
663 R, LaButti K, Egan R, Hajek P, Mukherjee S, Ovchinnikova G, Reddy TBK, Calhoun S,
664 Hayes RD, Rohwer RR, Zhou Z, Daum C, Copeland A, Chen I-MA, Ivanova NN, Kyrpides
665 NC, Mouncey NJ, del Rio TG, Grigoriev IV, Hofmeyr S, Oliker L, Yelick K,
666 Anantharaman K, McMahon KD, Woyke T, Eloe-Fadrosh EA. 2024. Coassembly and
667 binning of a twenty-year metagenomic time-series from Lake Mendota. Sci Data 11:966.

668 41. Buck M, Garcia SL, Fernandez L, Martin G, Martinez-Rodriguez GA, Saarenheimo J,
669 Zopfi J, Bertilsson S, Peura S. 2021. Comprehensive dataset of shotgun metagenomes from
670 oxygen stratified freshwater lakes and ponds. Sci Data 8:131.

671 42. Hädrich A, Heuer VB, Herrmann M, Hinrichs K-U, Küsel K. 2012. Origin and fate of
672 acetate in an acidic fen. FEMS Microbiol Ecol 81:339–354.

673 43. Roden EE, Wetzel RG. 1996. Organic carbon oxidation and suppression of methane
674 production by microbial Fe(III) oxide reduction in vegetated and unvegetated freshwater
675 wetland sediments. Limnol Oceanogr 41:1733–1748.

676 44. Roden EE, Wetzel RG. 2003. Competition between Fe(III)-reducing and methanogenic
677 bacteria for acetate in iron-rich freshwater sediments. Microb Ecol 45:252–258.

678 45. Reiche M, Torburg G, Küsel K. 2008. Competition of Fe(III) reduction and methanogenesis
679 in an acidic fen. FEMS Microbiol Ecol 65:88–101.

680 46. Teh YA, Dubinsky EA, Silver WL, Carlson CM. 2008. Suppression of methanogenesis by
681 dissimilatory Fe(III)-reducing bacteria in tropical rain forest soils: implications for
682 ecosystem methane flux. Glob Change Biol 14:413–422.

683 47. Stookey LL. 1970. Ferrozine—a new spectrophotometric reagent for iron. Anal Chem
684 42:779–781.

685 48. Riemer J, Hoepken HH, Czerwinska H, Robinson SR, Dringen R. 2004. Colorimetric
686 ferrozine-based assay for the quantitation of iron in cultured cells. Anal Biochem 331:370–
687 375.

688 49. Babraham Bioinformatics. FastQC a quality control tool for high throughput sequence data.
689 http://www.bioinformatics.babraham.ac.uk/projects/fastqc/

690 50. Krueger F. Trim Galore. The Babraham Institute.
691 https://github.com/FelixKrueger/TrimGalore

692 51. Martin M. 2011. Cutadapt removes adapter sequences from high-throughput sequencing
693 reads. 1. EMBnet.journal 17:10–12.

694 52. Kopylova E, Noé L, Touzet H. 2012. SortMeRNA: fast and accurate filtering of ribosomal
695 RNAs in metatranscriptomic data. Bioinformatics 28:3211–3217.

696 53. Langmead B, Salzberg SL. 2012. Fast gapped-read alignment with Bowtie 2. Nat Methods
697 9:357–359.

698 54. Li H, Handsaker B, Wysoker A, Fennell T, Ruan J, Homer N, Marth G, Abecasis G, Durbin
699 R, 1000 Genome Project Data Processing Subgroup. 2009. The sequence alignment/map
700 format and SAMtools. Bioinforma Oxf Engl 25:2078–2079.

701 55. Anders S, Pyl PT, Huber W. 2015. HTSeq—a Python framework to work with high-
702 throughput sequencing data. Bioinformatics 31:166–169.

703 56. R Core Team. 2024. R: A Language and Environment for Statistical Computing. R
704 Foundation for Statistical Computing, Vienna, Austria.

705 57. Posit team. 2023. RStudio: Integrated Development Environment for R (1.4.1717). Posit
706 Software, PBC, Boston, MA.

707 58. Love MI, Huber W, Anders S. 2014. Moderated estimation of fold change and dispersion
708 for RNA-seq data with DESeq2. Genome Biol 15:550.

709 59. Gilchrist CLM, Booth TJ, van Wersch B, van Grieken L, Medema MH, Chooi Y-H. 2021.
710 cblaster: a remote search tool for rapid identification and visualization of homologous gene
711 clusters. Bioinforma Adv 1:vbab016.

712 60. Gilchrist CLM, Chooi Y-H. 2021. clinker & clustermap.js: automatic generation of gene
713 cluster comparison figures. Bioinformatics 37:2473–2475.

714 61. Yu NY, Wagner JR, Laird MR, Melli G, Rey S, Lo R, Dao P, Sahinalp SC, Ester M, Foster
715 LJ, Brinkman FSL. 2010. PSORTb 3.0: improved protein subcellular localization prediction
716 with refined localization subcategories and predictive capabilities for all prokaryotes.
717 Bioinformatics 26:1608–1615.

718 62. Shen H-B, Chou K-C. 2010. Gneg-mPLoc: A top-down strategy to enhance the quality of
719 predicting subcellular localization of Gram-negative bacterial proteins. J Theor Biol
720 264:326–333.

721 63. Bernhofer M, Dallago C, Karl T, Satagopam V, Heinzinger M, Littmann M, Olenyi T, Qiu
722 J, Schütze K, Yachdav G, Ashkenazy H, Ben-Tal N, Bromberg Y, Goldberg T, Kajan L,
723 O'Donoghue S, Sander C, Schafferhans A, Schlessinger A, Vriend G, Mirdita M, Gawron
724 P, Gu W, Jarosz Y, Trefois C, Steinegger M, Schneider R, Rost B. 2021. PredictProtein -
725 predicting protein structure and function for 29 years. Nucleic Acids Res 49:W535–W540.

726 64. Jones P, Binns D, Chang H-Y, Fraser M, Li W, McAnulla C, McWilliam H, Maslen J,
727 Mitchell A, Nuka G, Pesseat S, Quinn AF, Sangrador-Vegas A, Scheremetjew M, Yong S-
728 Y, Lopez R, Hunter S. 2014. InterProScan 5: genome-scale protein function classification.
729 Bioinformatics 30:1236–1240.

730 65. Blum M, Chang H-Y, Chuguransky S, Grego T, Kandasaamy S, Mitchell A, Nuka G,
731 Paysan-Lafosse T, Qureshi M, Raj S, Richardson L, Salazar GA, Williams L, Bork P,
732 Bridge A, Gough J, Haft DH, Letunic I, Marchler-Bauer A, Mi H, Natale DA, Necci M,
733 Orengo CA, Pandurangan AP, Rivoire C, Sigrist CJA, Sillitoe I, Thanki N, Thomas PD,
734 Tosatto SCE, Wu CH, Bateman A, Finn RD. 2021. The InterPro protein families and
735 domains database: 20 years on. Nucleic Acids Res 49:D344–D354.